

C-N and C-O Bonds Formation in Copper-Catalyzed/ Mediated sp^3 C-H Activation: Mechanistic Studies from Experimental and Computational Aspects

Yuhang Yang, Fei Cao, Linbin Yao, Tao Shi, Bencan Tang, Yoichiro Kuninobu, and Zhen Wang

J. Org. Chem., **Just Accepted Manuscript** • DOI: 10.1021/acs.joc.0c01038 • Publication Date (Web): 17 Jul 2020

Downloaded from pubs.acs.org on July 17, 2020

Just Accepted

“Just Accepted” manuscripts have been peer-reviewed and accepted for publication. They are posted online prior to technical editing, formatting for publication and author proofing. The American Chemical Society provides “Just Accepted” as a service to the research community to expedite the dissemination of scientific material as soon as possible after acceptance. “Just Accepted” manuscripts appear in full in PDF format accompanied by an HTML abstract. “Just Accepted” manuscripts have been fully peer reviewed, but should not be considered the official version of record. They are citable by the Digital Object Identifier (DOI®). “Just Accepted” is an optional service offered to authors. Therefore, the “Just Accepted” Web site may not include all articles that will be published in the journal. After a manuscript is technically edited and formatted, it will be removed from the “Just Accepted” Web site and published as an ASAP article. Note that technical editing may introduce minor changes to the manuscript text and/or graphics which could affect content, and all legal disclaimers and ethical guidelines that apply to the journal pertain. ACS cannot be held responsible for errors or consequences arising from the use of information contained in these “Just Accepted” manuscripts.

C-N and C-O Bonds Formation in Copper-Catalyzed/Mediated sp^3 C-H Activation: Mechanistic Studies from Experimental and Computational Aspects

Yuhang Yang,^{[a],‡} Fei Cao,^{[b],‡} Linbin Yao,^{[c],‡} Tao Shi,^[a] Bencan Tang,^{*[c]} Yoichiro Kuninobu,^{*[d]} and Zhen Wang^{*[a,b]}

^[a]School of Pharmacy, Lanzhou University, West Donggang Road No. 199, Lanzhou 730000, Gansu, China

^[b]State Key Laboratory of Applied Organic Chemistry, Lanzhou University, Lanzhou 730000, Gansu, China

^[c]Department of Chemical and Environmental Engineering, Faculty of Science and Engineering, The University of Nottingham Ningbo China, 199 Taikang East Road, Ningbo 315100, China

^[d]Institute for Materials Chemistry and Engineering, Kyushu University, 6-1 Kasugakoen, Kasuga-shi, Fukuoka 816-8580, Japan

KEYWORDS amidation • acetoxylation • concerted metalation-deprotonation • C-H activation • density functional calculations

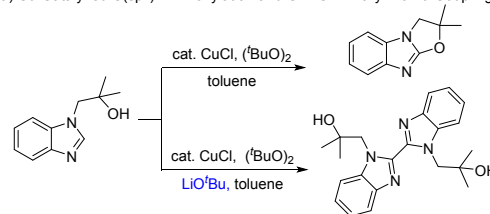
ABSTRACT: Mechanistic studies on Cu-catalyzed/mediated sp^3 C-H amidation and acetoxylation are investigated from experimental and computational aspects. The concerted metalation-deprotonation (CMD) mechanism rather than a radical-involved pathway is proved to occur in amidation and acetoxylation reactions, and this is the rare example of CMD mechanism involved in the more challenging sp^3 C-H activations. Theoretical calculations demonstrated that CMD is the rate determining step either for methylic or benzylic positions in amidation and acetoxylation reactions, and intermolecular nucleophilic addition of acetate anions is more favorable than ring-opening of β -lactam and intramolecular acetoxylation. These mechanistic researches on the divergent and condition-dependent product formation are critical for developing Cu-promoted C-H functionalization via CMD mechanism.

INTRODUCTION

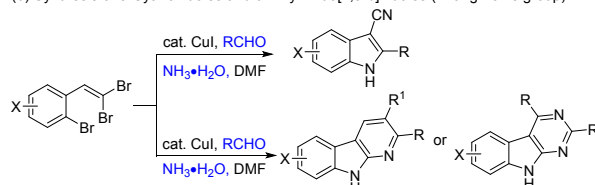
A product switching by changing reaction parameters, such as solvents and anions, when using the same transition metal catalyst and substrates in each reaction, is an interesting phenomenon. Although such divergent transformations are powerful tools to synthesize different types of compounds, the exploration of such transformations is still insufficient.¹⁻⁴ As several recent examples of product switching reactions, Cu-catalyzed C(sp^2)-H alkoxylation and C-H/C-H biaryl homo-coupling (Kanai's group)⁵ Cu-catalyzed synthesis of 3-cyanoindoles and 9H-pyrimido[4,5-b]indoles by changing the equivalents of aldehydes and concentration of ammonia (Scheme 1b),⁶ and Brønsted base-switched selective mono- and dithiolation of benzamides under Cu catalysis (Scheme 1c)⁷ have been reported. We reported Cu(OAc)₂-catalyzed C(sp^3)-H/C(sp^2)-H amidation⁸⁻⁹ and Cu(OAc)₂-mediated C(sp^3)-H acetoxylation.¹⁰⁻¹¹ The reactions can be switched by changing the solvents and bases whereas the same copper salt and substrates are used. These reactions are the rare examples of solvent- and/or base-controlled product switching reactions.

Scheme 1. Examples of product switching reactions

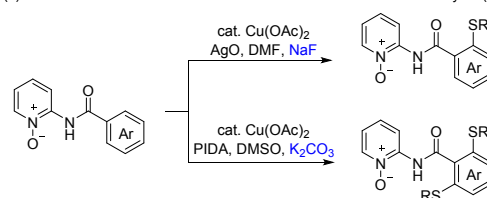
(a) Cu-Catalyzed C(sp^2)-H Alkoxylation and C-H/C-H Biaryl Homo-Coupling (Kanai's group)



(b) Synthesis of 3-Cyanoindoles and 9H-Pyrimido[4,5-b]indoles (Zhang-Fan's group)

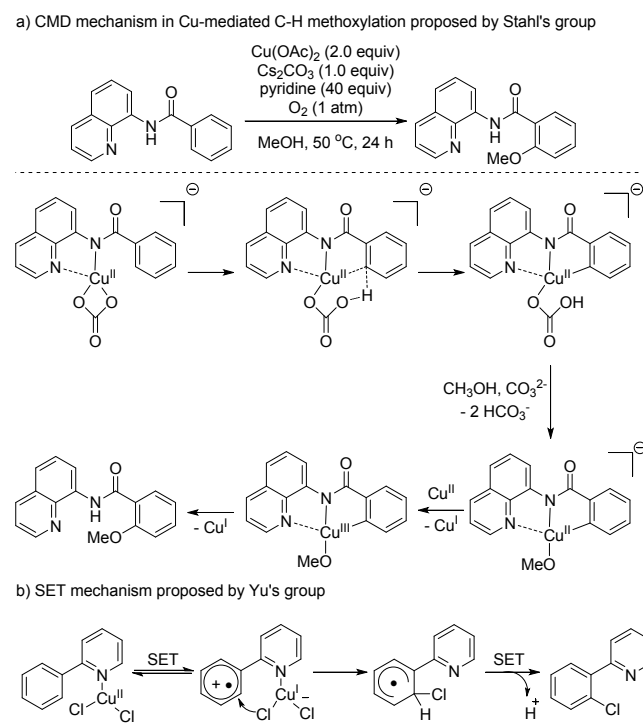


(c) Brønsted Base-Switched Mono- and Dithiolation under Cu Catalysis (Wang's group)



In recently reported first-row transition-metal-catalyzed C-H functionalization reactions, some C-H bonds cleavage occur via a concerted metalation-deprotonation (CMD) mechanism, in which metalation and intramolecular deprotonation proceed simultaneously.^{1,12} One of the most comprehensive mechanistic studies was reported by Stahl in the Cu(II)-mediated C(sp²)-H methoxylation. In Stahl's mechanism, Cu(II) and Cu(III) species participate in the C(sp²)-H activation and the subsequent reductive elimination steps, respectively (**Scheme 2a**).¹ The mechanism is totally different from a radical involved single-electron transfer (SET) mechanism reported by Yu's group for the explanation of the C(sp²)-H chlorination (**Scheme 2b**).¹³⁻¹⁴ Notably, the recently reported mechanistic studies mainly have focused on sp² C-H functionalizations, in-depth studies on more challenging sp³ C-H functionalizations are still in infancy and worth exploring.¹² We herein report mechanistic studies on our reported Cu(OAc)₂-catalyzed C(sp³)-H/C(sp²)-H amidation and Cu(OAc)₂-mediated C(sp³)-H acetoxylation from experimental and computational aspects.

Scheme 2. Previously reported mechanism in Cu-mediated C-H bond activation



RESULTS AND DISCUSSION

1. Mechanistic studies on C-N formation

Considering that radical pathways and two-electron transfer manifolds via organometallic C-Cu intermediates are two kinds of mechanisms commonly proceeded in Cu-promoted C-H activation,^{12,15-17} we postulated that the mechanism of our proposed C-H amidation and acetoxylation may be inseparable from the above two types of mechanism.

1.1 Exclusion of the radical pathway on C-N formation

At the beginning, we focused our concentration on verifying the radical pathway mainly from the following three aspects: **(1) Electronic effects of substituents:** substrates bearing an electron-donating or -withdrawing substituent on the benzene ring **1a-1d** were tested under the optimized C-H amidation conditions, and the overall yields of amidated products were similar to each other. (**Table 1**). These results indicated that amidation did not proceed via the radical pathway because electron-deficient aromatics should not be easily oxidized compared with electron-rich ones.¹³⁻¹⁴ **(2) Hammett plot of amidation:** the rates were faster for substrates with electron-withdrawing groups on the aromatic rings, and the slope calculated by a Hammett plot using σ_{para} values was 0.70 (**Figure 1, Tables S1 and S2, Figure S1**). The positive slope revealed that amidation did not proceed via a radical mechanism for electron-rich groups were more beneficial to the reaction rates in radical-involved pathway than electron-deficient ones.¹³⁻¹⁴ **(3) Effect of the radical inhibitor:** 1-3 equivalents of the radical scavenger TEMPO, did not influence the yields of amidated products, further excluding the possibility of a radical pathway (**Table 2**).

Table 1. Electronic effects of substituents on C-H amidation

entry	substrate	X	2 (%) ^[a]	3 (%) ^[a]	overall yield(%)
1	1a	OMe	53	36	89
2	1b	H	57	37	94
3	1c	Cl	47	44	91
4	1d	F	48	47	95

[a] Yields were determined by ¹H NMR.

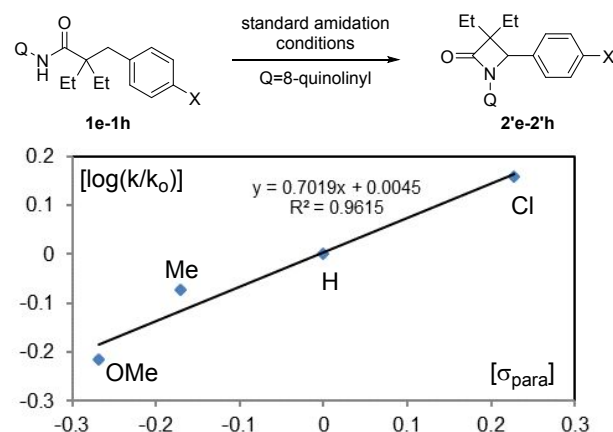
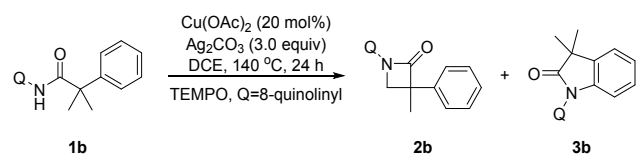


Figure 1. Hammett plot of **1e-1h**

Table 2. Effect of the radical inhibitor (TEMPO)


entry	solvent	TEMPO (equiv)	2b (%) ^[a]	3b (%) ^[a]	overall yield(%)
1	DCE	0	58	32	90
2	DCE	1.0	58	31	89
3	DCE	2.0	60	25	85
4	DCE	3.0	63	28	91

[a] Yields were determined by ¹H NMR.

1.2 Verification of the possibility of CMD pathway

Since the radical pathway in C-H amidation has been denied by the above experiments, moreover, the organometallic C-H activation pathways also typically favor electron-rich substrates, albeit to a less extent than radical reactions,^{1,18} thus we considered the CMD mechanism may be more plausible, because CMD supporting electron-deficient substrates has been reported.^{1,19-28}

1.2.1 Kinetic isotope effect in C(sp³)-N formation

A powerful technique especially suitable for studying reaction mechanisms of C-H bond functionalization—kinetic isotope effect (KIE), was measured to provide information on whether C-H bond cleavage was included in the rate determining step (RDS). The KIE values of C(sp³)-H amidation were measured by the following three ways: (1) C(sp³)-H amidation reactions of non-deuterated and deuterated substrates were tested independently in parallel tubes, and the KIE value was 2.4 (**Scheme 3a**, **Scheme 3. KIE experiments for C(sp³)-H amidation**

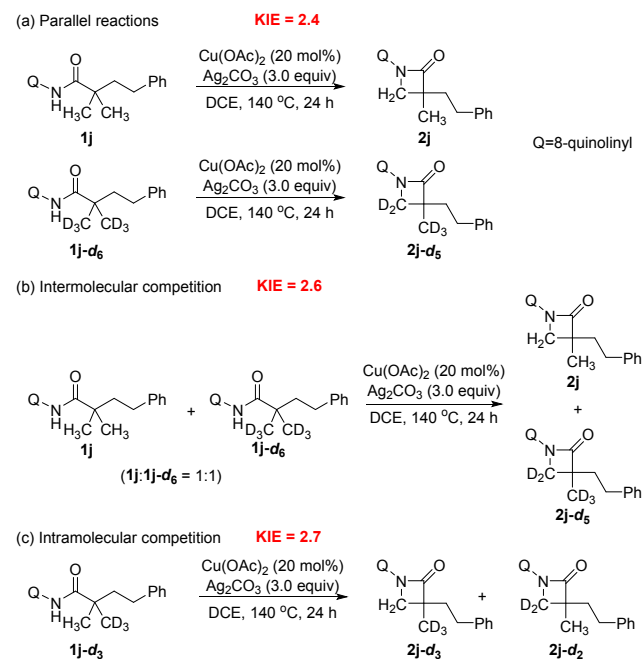


Table S3 and Figure S2); (2) intermolecular competitive C(sp³)-H amidation reaction of a mixture of non-deuterated and deuterated substrates was studied in one tube, and the KIE value was 2.6 (**Scheme 3b**, **Table S4 and Figure S3**); (3) intramolecular competitive C(sp³)-H amidation of substrate bearing one CH₃ and one CD₃ groups simultaneously was carried out, and the KIE value was 2.7 (**Scheme 3c**, **Table S5 and Figure S4**). Taken the above three experiments together, C(sp³)-H activation may occur during the rate-determining step,²⁹ and this is consistent with the positive Hammett slope observed for reactions in which C-H deprotonation contributes strongly to the transition state,¹ indicating the possibility of CMD mechanism in amidation.

1.2.2 Reaction orders of amides and Cu(OAc)₂ in C(sp³)-N formation.

To further clarify the mechanism, we investigated reaction orders of amides (**Figure 2**, **Tables S6-7**, **Figures S5-6**) and Cu(OAc)₂ (**Figure 2**, **Tables S8-9**, **Figures S7-8**) in C(sp³)-N formation. The rates showed a first-order dependence on concentrations of amides and Cu(OAc)₂, which indicated that Cu-catalyzed C-H activation was the likely rate-determining step. This experiment provided another evidence for CMD-involved C(sp³)-N formation.

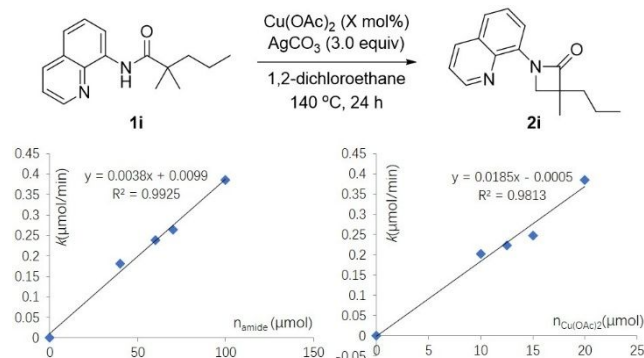
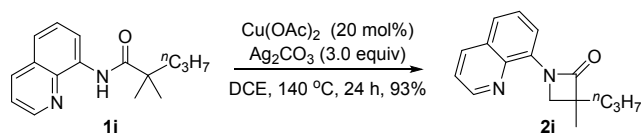


Figure 2. Reaction orders of amides and Cu(OAc)₂ in C(sp³)-N formation.

1.2.3 Investigation of the importance of acetate and carbonate anions in C(sp³)-N formation.

According to the previous reports, acetate and carbonate anions have been proved to be beneficial in the organometallic C-H activation,^{1,7,22,30-33} thus we intended to verify the CMD mechanism by elucidating the importance of acetate and carbonate anions in C(sp³)-H amidation.

To verify the importance of carbonate anions, several silver salts with various anions were firstly screened in the premise of using 20 mol% of Cu(OAc)₂ as the catalyst. However, all tested anions gave **2i** in rather low yields (**Table 3**, entries 1-6), demonstrating the importance of carbonate anions in C-H amidation. Since the necessity of carbonate anions in C-H amidation have been proved, then carbonate anions contained Cu₂(OH)₂CO₃³⁴ replacing Cu(OAc)₂ was employed to evaluate the significance of acetate anions. As a result, **2i** was not detected, albeit the mixture contained carbonate anions (entry 7), which implied there maybe another factor besides carbonate anions infecting the amidation. In the case of using a mixture of Cu₂(OH)₂CO₃ and AgOAc, the reaction

Table 3. Investigation of the importance of acetate and carbonate anions.

entry	Ag salt	Cu	additive	2i (%) ^[a]
1	Ag ₃ PO ₄	Cu(OAc) ₂	-	15
2	AgOAc	Cu(OAc) ₂	-	3
3	AgO	Cu(OAc) ₂	-	12
4	Ag ₂ O	Cu(OAc) ₂	-	9
5	AgF	Cu(OAc) ₂	-	<1
6	AgF ₂	Cu(OAc) ₂	-	<1
7	Ag ₂ CO ₃	Cu ₂ (OH) ₂ (CO ₃)	-	<1
8	AgOAc	Cu ₂ (OH) ₂ (CO ₃)	-	6
9	AgOAc	Cu(OAc) ₂	-	3
10	AgOAc	Cu(OAc) ₂	K ₂ CO ₃ ^[b]	15
11	AgOAc	Cu(OAc) ₂	K ₂ CO ₃ ^[c]	21
12	AgOAc	Cu(OAc) ₂	K ₂ CO ₃ ^[d]	31
13	AgOAc	Cu(OAc) ₂	K ₂ CO ₃ ^[e]	31

[a] Yields were determined by ¹H NMR. [b] 0.5 equiv of K₂CO₃. [c] 1.0 equiv of K₂CO₃. [d] 2.0 equiv of K₂CO₃. [e] 3.0 equiv of K₂CO₃.

proceeded whereas the yield of **2i** was 6% (entry 8), implying acetate anions may be beneficial to amidation. In addition, acetate anions contained AgOAc and Cu(OAc)₂ only gave 3% of the product (entry 9), but the yield could be improved by using K₂CO₃ as an additive and increasing the amount of K₂CO₃ (entries 10-13).

Judging from the above results, only Cu(OAc)₂ in concert with Ag₂CO₃ could generate the amidated product **2i** in the highest yield, identifying the significance of carbonate and acetate anions in amidation, and the species is similar to that of the reported C-H transformations via CMD mechanism.¹

1.2.4 Competitive benzylic and methylic C(sp³)-H bonds cleavage

With the desire to find more evidence(s) to support the CMD mechanism, the regioselectivity of C(sp³)-H amidation between competitive benzylic and methylic C(sp³)-H bonds was investigated. When various substrates with both benzyl and methyl groups located at the competitive β -positions of amides were subjected to the standard conditions, all substrates with an electron-donating or withdrawing group on the *para*-position of the aromatic ring gave both methylic and benzylic C(sp³)-H bond amidated products **2** and **2'** (Table 4). Judging from the facts that C(sp³)-H amidation was apt to occur at a more acidic benzylic site rather than a less hindered methyl group, C-H bond activation may involve in the key step. Subsequently, we conducted DFT calculation of substrates **1k-1q** to explain the regioselectivity between

competitive benzylic and methylic C(sp³)-H bonds amidation (*Vide infra*).

Taken the above KIE values, first-order dependence on concentrations of amides and Cu(OAc)₂, importance of acetate and carbonate anions and the tendency of amidation at the more acidic benzylic site together, CMD was proved to occur in C-N formation.

Table 4. Regioselectivity between competitive benzylic and methyl C(sp³)-H bonds in amidation

substrate	1k	1l	1m	1n	1o	1p	1q
	OMe	Me	H	Br	Cl	F	CF ₃
2 (%) ^[a]	25	38	25	25	26	30	21
2' (%) ^[a]	53	52	64	61	62	61	59
2/2'	0.47	0.73	0.39	0.41	0.42	0.49	0.36

[a] Yields were determined by ¹H NMR.

2. Mechanistic studies on C(sp³)-O formation and exploration of its correlations with C(sp³)-N formation

2.1 Substrate scope investigation and reaction conditions studies

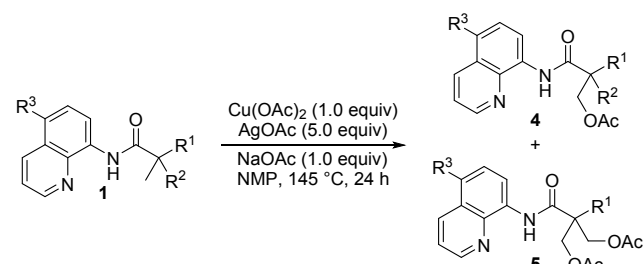
2.1.1 Substrate scope in C-O formation

We also reported copper-mediated C(sp³)-H acetoxylation (Table 5).¹⁰ Amides with a tertiary alkyl group generated the corresponding mono- and di-acetylated products **4r**, **4i-4j**, **4j-d₅** and **5r**, **5i-5j**, **5j-d₄** (entries 1-4). Notably, acetoxylation did not occur at the acidic benzylic C(sp³)-H bonds in the case of substrate **1j** (entry 3). The results of substrates **1s-1v** indicated that acetoxylation occurred preferentially at the methyl groups, and did not proceed at the terminal position of the ethyl groups, methylene moieties (internal position), or benzylic C(sp³)-H bonds (entries 5-8). The corresponding acetylated product **4w** was obtained in 68% yield for substrate **1w** bearing a methoxy group on the quinolinyl group (entry 9). The above examples showed the high functional group tolerance of Cu-mediated C(sp³)-H acetoxylation.

2.1.2 The amount of copper in C-N and C-O formation

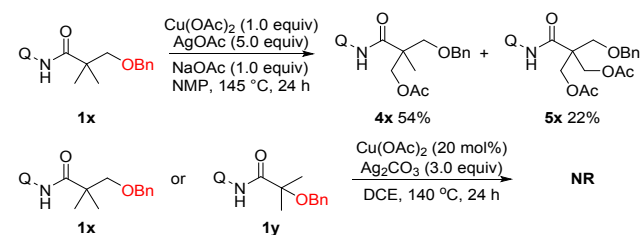
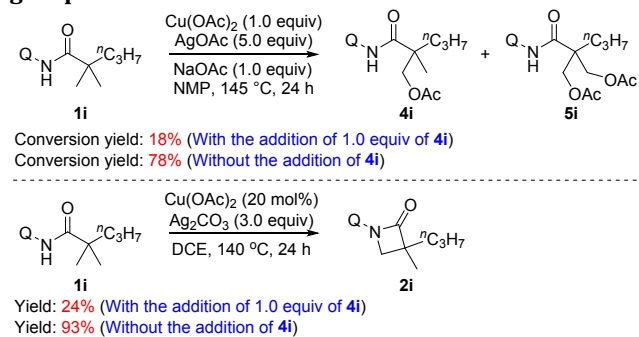
It is worth noting that β -hetero substituted substrate **1x** proceeded well in acetoxylation, but a tragic situation was observed in amidation in which the amidated product was not formed in detectable yield. In addition, the α -hetero substituted substrate **1y** gave a similarly frustrating result in amidation (Scheme 4). As for the different behaviors of substrate **1x** in amidation and acetoxylation, we hypothesized that the β -heteroatom as a Lewis base could coordinate with Cu atom deactivating Cu and further hindering the catalytic cycle of amidation, but the addition of stoichiometric quantities of Cu is adequate to prevent acetoxylation from being affected by the heteroatom.

In order to probe the coordination of heteroatoms, we examined acetoxylation and amidation of **1i** in the presence of acetylated amide **4i** (Scheme 5). As a result, 18% of substrate **1i** was transformed to a mixture of

Table 5. Investigation of Substrate Scope.^[a]

entry	4	yield (%) ^[b]	5	yield (%) ^[b]
1		4r 39		5r 38
2		4i 55		5i 23
3		4j 55		5j 21
4		4j-d5 51		5j-d4 18
5		4s 78		
6		4t 86		
7		4u 87		
8		4v 79		
9		4w 68		

[a] The data are cited from ref 10. [b] Isolated yields.

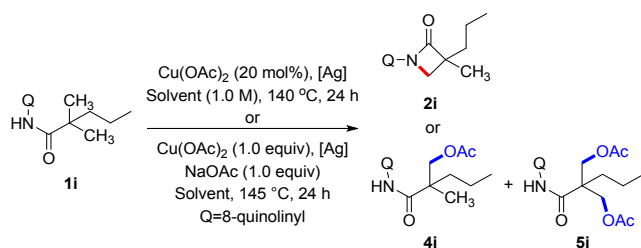
Scheme 4. Investigation of the inhibition effect of α/β -heteroatom on acetoxylation and amidation.**Scheme 5. Verification of the coordination of acetoxy group to Cu atom in C-N and C-O formation.**

mono- and di- acetoxyated products, and the conversion yield was much lower than that of the reaction without the addition of **4i** (78% conversion yield). In amidation, the yield of **2i** sharply diminished to 24% in the existence of **4i**, compared to the 93% yield observed in the absence of **4i**.

These results indicated that the stronger coordination ability of oxygen in acetoxy group of **4i** to the Cu center in a tridentate fashion than a bidentate starting substrate, could deactivate the catalytic activity of Cu salt,³⁵ resulting in the low yields of amidation and acetoxylation. This also reminds us that in normal situation the newly formed di-acetoxyated product is very likely to coordinate with Cu in a tetradentate manner, which is like the tridentate manner of mono-acetoxyated product, just because the coordination of product to catalyst is masked by the addition of stoichiometric quantities copper in acetoxylation. While in amidation, in the premise of without other heteroatom existed in the substrates, the weak coordination ability of previously formed amidated products would not affect the subsequent amidation, thus catalytic amount of Cu is adequate to amidation.

2.1.3 Comparison of the reactivity differences between C-H amidation and acetoxylation

Since catalytic amount of copper has been proved to be adequate in amidation conditions, could the amidation occur in the stoichiometric quantities copper contained acetoxylation conditions? In addition, we wonder know if there is any correlation between C-H amidation and acetoxylation. Therefore, substrate **1i** was then subjected to the conditions of C-H amidation and C-H acetoxylation (**Table 6**). In the case of using 1,2-dichloroethane as the solvent, the amidated product **2i** was obtained in 93% with no detection of the acetoxyated products **4i** when using 3 equiv AgCO_3 and 20 mol% Cu(OAc)_2 , while only 3% of the acetoxyated product **4i** was formed with no company of **2i** in the combination of 5 equiv AgOAc and 1 equiv Cu(OAc)_2 . In the case of employing NMP as the solvent, the mono- and di- acetoxyated products were obtained in a combined yield of 78% in the presence of 5 equiv AgOAc and 1 equiv Cu(OAc)_2 , in which the amidated product **2i** was not formed. On the other hand, 8.3% of the amidated product **2i** was provided in the presence of 3 equiv AgCO_3 and 20 mol% Cu(OAc)_2 , similarly, with no formation of the mono- and di- acetoxyated products. These results elaborated that a combination of Ag_2CO_3 and DCE was beneficial in giving the amidated products, whereas a cooperation of AgOAc and NMP was better for

Table 6. Comparison of the reactivity differences between C-H amidation and acetoxylation.

Solvent	Oxidant	
	Ag ₂ CO ₃ (3 equiv) ^[a]	AgOAc (5 equiv) ^[b]
DCE	2i = 93% ^[c]	4i = 3% ^[c]
NMP	2i = 8.3% ^[c]	4i : 5i = 55 % : 23% ^[c]

[a] 20mol% of Cu(OAc)₂ was used. [b] 1 equiv of Cu(OAc)₂ was used. [c] Yields were determined by ¹H NMR.

rendering the acetoxylation products. In other words, amidation could not occur in the acetoxylation condition and acetoxylation would not happen in the amidation conditions.

2.2 Regioselectivity between a more acidic benzylic and a less hindered methylic C(sp³)-H bonds in C-O formation

Another kind of special substrates were then investigated to reveal the regioselectivity between competitive benzylic and methylic C(sp³)-H bonds in C-H acetoxylation. The yields of the acetoxylation products enhanced with an increase in the electron-withdrawing ability of the functional group, indicating the acetoxylation reaction may not proceed via a SET mechanism and further supporting the CMD pathways in acetoxylation. In addition, whether the electron-donating or -withdrawing groups at the *para*-position of the aromatic ring, absolutely selectivity toward the less hindered β-methyl site over a more acidic β-benzylic site was observed, suggesting that the steric effect rather than electronic effect determined the distribution of final products. Unexpectedly, the selectivity in acetoxylation was in sharp contrast to the C-H amidation (Table 7).

This prompted us to propose an interaction mode, which is different from the intramolecular interaction in amidation, intermolecular nucleophilic addition of acetate anions to the CMD intermediate or the four-membered

Table 7. Regioselectivity between competitive benzylic and methylic C(sp³)-H bonds in C-H acetoxylation.

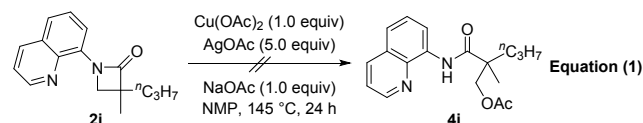
substrate	1k	1l	1m	1n	1o	1p	1q
	OMe	Me	H	Br	Cl	F	CF ₃
4 (%) ^[a]	67	71	74	62	78	81	83
4' (%) ^[a]	<1	<1	<1	<1	<1	<1	<1

[a] Yields were determined by ¹H NMR.

amidated product to render the acetoxylation products. To provide evidence for the above proposal, experiment and calculation were respectively conducted to verify the possibility of ring-opening of four-membered amidated products and the intermolecular addition of acetate anions to the CMD intermediate. In addition, the regioselectivity in acetoxylation was also clarified via calculation (*Vide infra*).

2.3 Exploration of the possibility of forming C-O bonds via cleavage of C-N bonds.

In order to explore if the β-lactam ring could open under the standard acetoxylation conditions to form the acetoxylation product, amidated product **2i** was directly subjected to the standard conditions of C-H acetoxylation (Equation (1)), nevertheless, the desired acetoxylation product **4i** was not detected at all. This result denied the formation of acetoxylation product involving ring-opening of the amidated product.



3. Computational analysis on CMD process and the subsequent C-N/C-O bonds formation

DFT calculation was conducted in Gaussian 09³⁶ to find more evidences for the CMD process the subsequent C-N/C-O bonds formation. Cu(II) species **Int₀** was considered as the zero point in these energy profiles, as some similar structures of **Int₀** has been reported.¹²

Started from **Int₀**, oxidation of which with AgOAc to provide **Int₁** was downhill and uphill by 0.6 kcal/mol in DCE and NMP, respectively (Figure 3). In this mechanism, formation of **Int₂** involved a deprotonation of the C(sp³)-H by the acetate ligand with concomitant Cu-C bond formation, analogous to the organometallic intermediates reported for Cu^{II} or Pd^{II}-promoted C-H activation reactions.^{1,22,33} The activation free energy for this step was 25.1 kcal/mol in DCE or 25.4 kcal/mol in NMP, which was similar to that of deprotonation of the arene C-H bond by the carbonate ligand on a Cu(II) species, where 25.9 kcal/mol was reported,¹ but was different with the energy barrier of 21.2 kcal/mol in the CMD process of C-H/N-H annulation of electron-deficient acrylamides with arynes reported by Zhang²⁸ and the energy barrier of 17.7 kcal/mol in the CMD process of amination of phenol derivatives with diarylamines demonstrated by Hirano and Miura as these are more acidic protons.³⁷

On the other hand, in many well-documented metal-promoted C-H functionalization reactions, stoichiometric Ag(I)-salts were often added to act as oxidants or to play additional roles in C-H activation,³⁸⁻⁴¹ so it is plausible to propose that AgOAc may also participate in the CMD process of this reaction. Indeed, our calculation suggested that a Ag involved CMD process was also energetically possible, for a Ag-contained complex **Int_{1Ag}** with a lower Gibbs free energy of 9.5 kcal/mol in NMP and 11.0 kcal/mol in DCE, relative to **Int₀**, was obtained when oxidation of **Int₀** with AgOAc, suggesting that this intermediate was stabilized by Ag coordination. The Gibbs

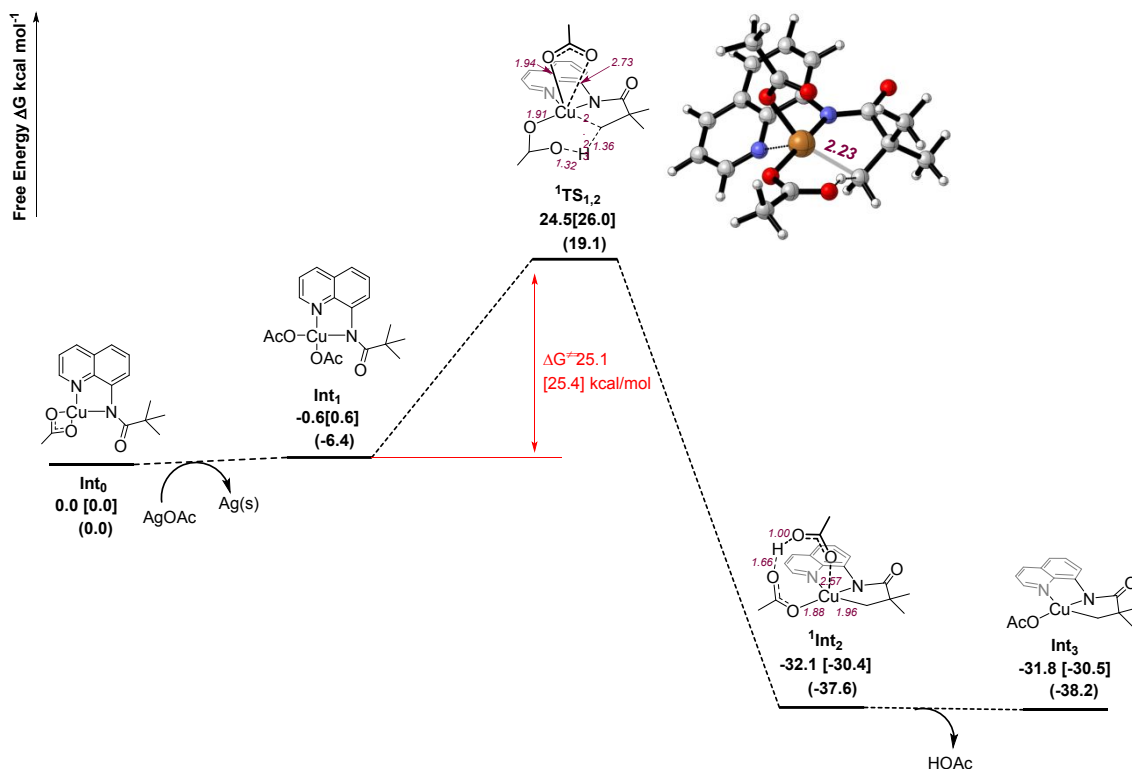


Figure 3. Computed free energy profile for CMD process. The relative free energies calculated in the gas phase with (U)B3LYP/6-31G(d)-SDD(Cu) are given in kcal/mol and presented in brackets. The relative free energies in DCE given in kcal/mol are calculated by PCM(DCE)-(U)B3LYP-d3(BJ)//6-311++G(d,p)-SDD (Cu) // (U)B3LYP/6-31G(d)-SDD(Cu). The relative free energies in NMP given in kcal/mol are calculated by PCM(DCE)-B3LYP- d3(BJ) //6-311++G(d,p)-SDD (Cu) // B3LYP/6-31G(d)-SDD(Cu), which are quoted in square brackets. Bond distance in Å. Molecular graphics for transition state structures were produced by CYLview.

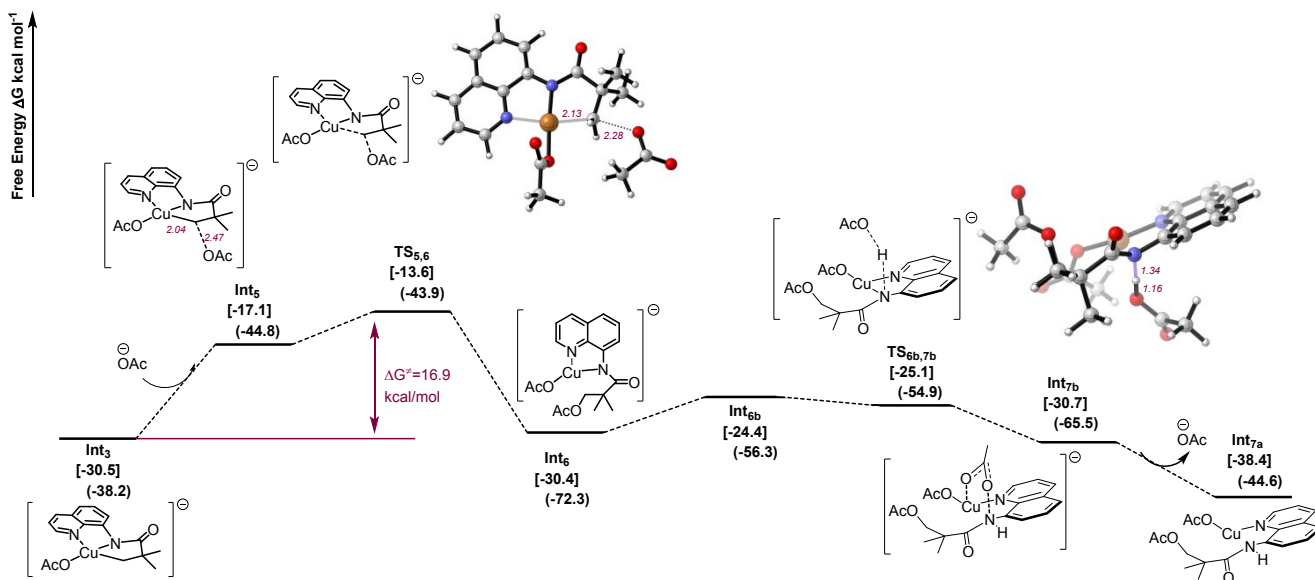


Figure 4. Computed free energy profile for acetoxylation. The relative free energies calculated in the gas phase with (U)B3LYP/6-31G(d)-SDD(Cu) are given in kcal/mol and presented in brackets. The relative free energies in DCE given in kcal/mol are calculated by PCM(DCE)-(U)B3LYP- d3(BJ)//6-311++G(d,p)-SDD (Cu) // B3LYP/6-31G(d)-SDD(Cu). The relative free energies in NMP given in kcal/mol are calculated by PCM(DCE)-B3LYP- d3(BJ) //6-311++G(d,p)-SDD (Cu) // B3LYP/6-31G(d)-SDD(Cu), which are quoted in square brackets. Bond distance in Å. Molecular graphics for transition state structures were produced by CYLview.

free activation energy of CMD process via $\text{TS}_{1,2\text{Ag}}$ was 25.2 kcal/mol relative to $\text{Int}_{1\text{Ag}}$ (as evaluated in DCE or NMP), which was approximately equal to the energy barriers without the assistance of Ag (**Figure S9**), indicating that Ag had negligible influence on the CMD, and further reminding us that Ag was likely to play more important roles in oxidizing Cu(II) to Cu(III) to participate in the CMD or/and Cu(I) to Cu(II) to recycle Cu.

After releasing AcOH from Int_2 (**Figure 3**) or AcOH and Ag from $\text{Int}_{2\text{Ag}}$ (**Figure S9**), Int_3 was formed. Acetoxylation of Int_3 may proceed via several possible pathways (**Figure S10**). Among them, intermolecular nucleophilic addition of acetate anions to metalacyclic intermediate Int_3 to give rise to acetoxylation products Int_6 was the most energetically favored (**Figures S10**). In addition, the energy barrier for intermolecular nucleophilic addition was 16.9 kcal/mol (in NMP, **Figures 4** and **S10**), which was 6.7 kcal/mol (in NMP) lower than the amidation process ($\Delta G^\ddagger = 23.6$ kcal/mol in NMP, **Figures 5**),⁴² and this outcome was in accordance with the phenomenon that acetoxylation product **4** could not be formed via ring-opening of amidated product (**Equation (1)**) since it must firstly conquer higher energy barrier than direct intermolecular acetoxylation. Subsequently, cleavage of Cu-N bond in Int_6 via $\text{TS}_{6\text{b},7\text{b}}$ and releasing acetate anions gave $\text{Int}_{7\text{a}}$ with a lower Gibbs free energy of 7.9 kcal/mol (in NMP) compared to Int_3 (**Figure 4**).

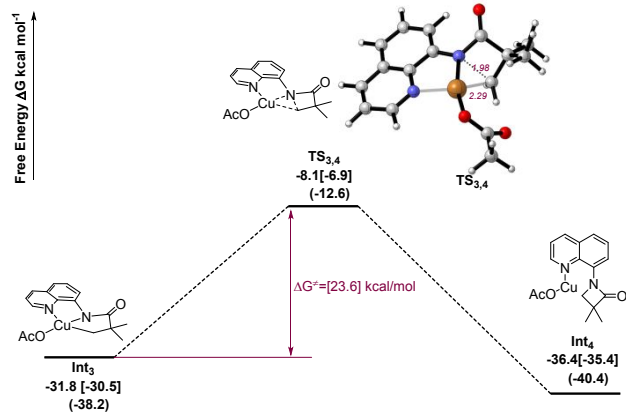


Figure 5. Computed free energy profile for amidation step. The relative free energies calculated in the gas phase with (U)B3LYP/6-31G(d)-SDD(Cu) are given in kcal/mol and presented in brackets. The relative free energies in DCE given in kcal/mol are calculated by PCM(DCE)-(U)B3LYP-d3(BJ)//6-311++G(d,p)-SDD (Cu) // B3LYP/6-31G(d)-SDD(Cu). The relative free energies in NMP given in kcal/mol are calculated by PCM(DCE)-B3LYP-d3/6-311++G(d,p)-SDD (Cu) // B3LYP/6-31G(d)-SDD(Cu), which are quoted in square brackets. Bond distance in Å. Molecular graphics for transition state structures were produced by CYLview.

Afterwards, we calculated the energy barriers of CMD and the subsequent C-N or C-O bonds formation in methylic or benzylic sites of substrates **1k-1q** to make clear the regioselectivity changes in amidation and acetoxylation (**Tables 8-9, Figures S11-14, Tables S13-23**). The results revealed that whether in amidation or acetoxylation, and whether in methylic or benzylic sites, CMD step with or without the assistance of Ag was the rate

determining step. The energy barriers of the CMD step of methylic and benzylic sites in amidation were similar to each other, as in the case that energy barriers of the subsequent C-N formation step of methylic and benzylic sites in amidation had slight difference, which could explain the phenomenon why both methylic and benzylic C-H bonds could be amidated. In the case of acetoxylation, there was negligible difference on the energy barriers of the CMD step of methylic and benzylic sites, but the energy barriers of the C-O formation step of benzylic sites were 6.3-6.8 kcal/mol higher than that of the methylic sites, we speculated this may be due to the fact that the high polarity of NMP and high concentration of ligand (acetate anions) made the surroundings of benzylic copper intermediate more crowded. Therefore, the lower energy barriers of the less hindered methylic sites could contribute to the absolute regioselectivities on methylic sites in acetoxylation.

Table 8. Computed free energy activation barriers for methyl and benzylic amidation.^[a]

Subst rate	$\Delta G^\ddagger_{\text{CMD methyl}}$	$\Delta G^\ddagger_{\text{CMD benzylic}}$	$\Delta G^\ddagger_{\text{C-N (2)}}$	$\Delta G^\ddagger_{\text{C-N (2')}}$	$\Delta\Delta G^\ddagger_{\text{CMD}}$
1k	27.6	25.3	22.2	18.2	2.3
1l	28.0	27.1	20.0	18.7	0.9
1m	27.6	26.9	21.2	19.8	0.7
1n	28.1	27.8	22.4	19.8	0.3
1o	27.7	27.3	22.5	20.0	0.4
1p	27.3	27.3	22.4	19.6	0.0
1q	27.8	28.0	22.5	20.7	-0.2

[a] The relative free energies in DCE given in kcal/mol are calculated by PCM(DCE)-(U)B3LYP-d3(BJ)/6-311++G(d,p)-SDD (Cu) // (U)B3LYP/6-31G(d)-SDD(Cu).

Table 9. Computed free energy activation barriers for methyl and benzylic acetoxylation.^[a]

Subst rate	$\Delta G^\ddagger_{\text{CMD Methyl}}$	$\Delta G^\ddagger_{\text{CMD Benzylic}}$	$\Delta G^\ddagger_{\text{C-O (4)}}$	$\Delta G^\ddagger_{\text{C-O (4')}}$	$\Delta\Delta G^\ddagger_{\text{CMD}}$	$\Delta\Delta G^\ddagger_{\text{C-O}}$
1k	[27.8]	[25.4]	[12.2]	[19.0]	2.4	-6.8
1l	[28.2]	[27.2]	[12.4]	[18.7]	1.0	-6.3
1m	[27.8]	[27.1]	[12.4]	[19.0]	0.7	-6.6
1n	[28.4]	[28.0]	[12.3]	[19.0]	0.4	-6.7
1o	[27.9]	[27.5]	[12.6]	[18.9]	0.4	-6.3
1p	[27.5]	[27.4]	[12.4]	[18.9]	0.1	-6.5
1q	[28.0]	[28.2]	[12.4]	[19.0]	-0.2	-6.6

[a] The relative free energies in NMP given in kcal mol⁻¹ are calculated by PCM(NMP)-B3LYP-d3(BJ) //6-311++G(d,p)-SDD (Cu) // B3LYP/6-31G(d)-SDD(Cu), which are quoted in square brackets.

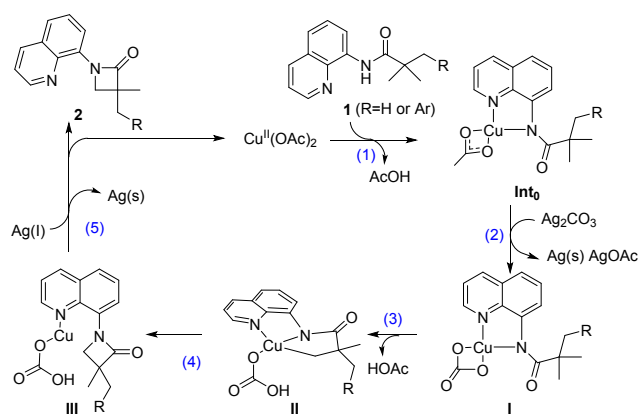
3. Proposed mechanism

3.1 Proposed mechanism for C-N formation

Based on the reported literatures¹² and the evidence above, we speculated the mechanism of C(sp³)-H

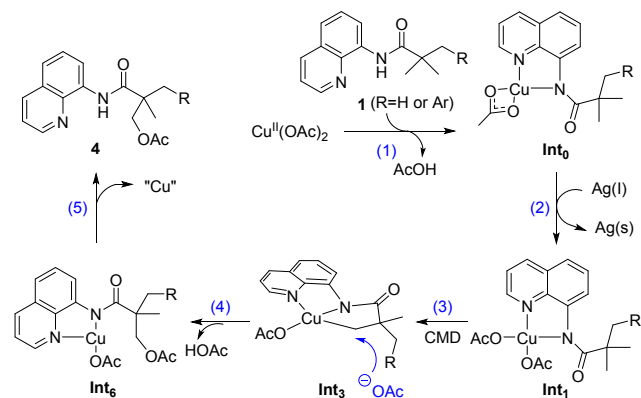
amidation and acetoxylation. The mechanism depicted in **Scheme 6** is for the formation of β -lactams: (1) coordination of substrate **1** to Cu^{II} species with the elimination of acetic acid generates intermediate **Int₀**; (2) oxidation of the copper intermediate **Int₀** with Ag_2CO_3 ⁴³ and ligand exchange to give intermediate **I** via leaving Ag and AgOAc free, the driving force for this step is that carbonate is dianion ligand; (3) formation of metalacyclic intermediate **II** was proceeded via a CMD pathway (C(sp³)-H bond activation),⁴⁴ which was supported by the necessity of acetate and carbonate anions, first order dependence on concentrations of $\text{Cu}(\text{OAc})_2$ and substrate, the large KIE value and positive Hammett slope; (4) subsequent C-N reductive elimination of $\text{Cu}(\text{III})$ contained **II** proceeds rendering $\text{Cu}(\text{I})$ contained **III**; and (5) oxidation of **III** with $\text{Ag}(\text{I})$ to give amidated product **2**.⁴³ However, the disproportionation of $\text{Cu}(\text{II})$ to form $\text{Cu}(\text{III})$ species could not be ruled out for mechanisms including $\text{Cu}(\text{II})$ disproportionation were also proposed in some C-H bond transformations.¹²

Scheme 6. Proposed mechanism for C(sp³)-H amidation



3.2 Proposed mechanism for C-O formation

The following mechanism is for the formation of acetoxyated product (**Scheme 7**): (1) coordination of substrate **1** to Cu^{II} species with elimination of acetic acid generates the identical intermediate with the amidation process; (2) oxidation of Cu^{II} with Ag salt to afford Cu^{III} species **Int₁**; (3) formation of metalacyclic intermediate **Int₃** via CMD pathway; (4) intermolecular nucleophilic attack of acetate on **Int₃** to form **Int₆**; (5) reductive elimination of Cu^{I} from **Int₆** to yield the acetoxyated product **4**.



addition of acetate anions to form **Int₆**, and this pathway was proved to be energetically the most favored one and thus the most likely pathway for the C-H acetoxylation in NMP; (5) dissociation of Cu species to liberate the acetoxyated product **4**, which is a stronger ligand than the starting material **1** thus leading to the necessity of stoichiometric copper salt. Notably, Ag -assisted CMD process was also proved to be energetically feasible in both C-N and C-O formation reactions.

CONCLUSION

In summary, we conducted experimental and computational experiments to elucidate the detailed mechanisms of our reported Cu -catalyzed intramolecular sp^3/sp^2 C-H amidation and Cu -mediated sp^3 C-H acetoxylation. It was identified that the $\text{Cu}(\text{II})$ -catalyzed or mediated C-H activation occurred via a CMD mechanism, and this is the rare example of CMD involving in the more challenging sp^3 C-H activation. The theoretical calculations revealed that whether in amidation or acetoxylation, and whether in methylic or benzylic sites, CMD step with or without the assistance of Ag was the rate determining step, and intermolecular nucleophilic addition of acetate anions was energetically more favorable over ring-opening of β -lactams or intramolecular acetoxylation. These mechanistic researches of the divergent and condition-dependent product formation are critical for developing Cu -promoted C-H functionalization via CMD mechanism.

EXPERIMENTAL SECTION

General information

All reactions were carried out in a dry solvent under argon atmosphere unless otherwise noted. $[\text{Cu}(\text{OAc})_2]$ (purity: 99.99%) was purchased from Aldrich Co. Solvents and silver salts were purchased from Wako Pure Chemical Industries, solvents were dried and degassed before use. Heating mantle was used as the heat source for all reactions requiring heating. NMR Spectra were recorded on JEOL ECX500 (500 MHz for ¹H NMR and 126 MHz for ¹³C NMR) and JEOL ECS400 (400 MHz for ¹H NMR and 101 MHz for ¹³C NMR) spectrometer. Proton chemical shifts are reported relative to a residual solvent peak (CDCl_3 at 7.26 ppm or TMS at 0 ppm). Carbon chemical shifts are reported relative to a residual solvent peak (CDCl_3 at 77.26 ppm). The following abbreviations were used to designate multiplicities: s = singlet, d = doublet, t = triplet, q = quartet, quint = quintet, m = multiplet, br = broad. IR spectra were recorded on a JASCO FT/IR-410. High-resolution mass spectra (HRMS) were measured on a JEOL JMS-T100LC AccuTOF spectrometer (for HRMS).

The spectra of amides **1b**,⁸ **1i**,¹⁰ **1j-1q**,⁸ **1j-d₆**,⁸ **1r-1x**¹⁰ and compounds **2b**,⁸ **2j-2q**,⁸ **2j-d₅**,⁸ **2'k-2'q**,⁸ **3b**,⁸ **4i-4x**,¹⁰ **4j-d₅**,¹⁰ **5i-5j**,¹⁰ **5r**,¹⁰ **5x**¹⁰ have been reported in our previous study. Compounds **1c-1d**,⁴⁵ **1f**,⁴⁶ **1g**,⁴⁷ **1h**⁴⁶ and **2'f-2'h**⁴⁶ were known compounds.

Statement for the kinetic data

In our experience, the yields of amidation or acetoxylation reactions were low when the reactions were stirred for 24 h at temperature that was below the optimal one, while the yields would be satisfactory only if the

reaction temperatures were up to the optimal conditions, indicating an induction period may be existed before the steady stage. On the other hand, the kinetic data in the supporting information, in which all of the runs exhibit non-zero y-intercepts, would be regarded as another evidence to support the existence of induction period. We speculated the reasons of the above-mentioned phenomenon may be considered as follows: in both amidation and acetoxylation reactions, the C-H activation step has been proposed as the rate determining step (RDS). That is, energy provided must be adequate to conquer the energy barriers of this key step to promote the advance of these two reactions. In the process of temperature rising, in which the temperatures of reaction systems were below the optimal one, it seems to be difficult to provide sufficient energy to conquer the barriers of RDS, thus maybe blocking the progress of reactions and ultimately resulting in the appearance of an induction period. On the other hand, Cu(III) was proposed to participate in the CMD step, thus the oxidation of Cu(II) to Cu(III) should happen before the CMD step. In conclusion, the processes of catalyst activation by ligand, oxidation of Cu(II) to Cu(III), and temperatures rise would take some time and result in the low reaction rates at the initial stage, therefore leading to the appearance of induction period.

General synthetic procedure for compounds 2a-2d, 2'e-2'h, 2i-2q, 2'k-2'q, 2j-d₂, 2j-d₃, 2j-d₅ and 3a-3d

A screw cap vial was charged with substrate **1** (0.10 mmol), Cu(OAc)₂ (3.63 mg, 20.0 μmol), Ag₂CO₃ (82.7 mg, 0.30 mmol), and solvent (1.0 mL) under Ar atmosphere. The vial was sealed and stirred vigorously at 140 °C for 24 h. Then the reaction mixture was cooled to room temperature, filtered through a pad of Celite and concentrated in vacuo. The residue was directly analyzed by ¹H NMR using 1,1,2,2-tetrachloroethane as the internal standard to determine the yields of products or purified by column chromatography on silica gel (hexane/ethyl acetate = 8:1) to give the desired products.

Procedure for a gram-scale amidation reaction for synthesizing 2j.

A screw cap vial was charged with substrate **1j** (1.40 g, 4.40 mmol), Cu(OAc)₂ (175.8 mg, 0.88 mmol), Ag₂CO₃ (3.64 g, 13.2 mmol), and solvent (44.0 mL) under Ar atmosphere. The vial was sealed and stirred vigorously at 140 °C for 24 h. Then the reaction mixture was cooled to room temperature, filtered through a pad of Celite and concentrated in vacuo. The residue was directly purified by column chromatography on silica gel (hexane/ethyl acetate = 8:1) to give **2j** (1.0 g, 73% yield) as a yellow oil.

General synthetic procedure for compounds 4i-4q, 4j-d₅, 4r-4x, 5i-5j, 5r, 5x and 5j-d₄

A mixture of substrate **1** (0.10 mmol), Cu(OAc)₂ (18.2 mg, 0.10 mmol), NaOAc (8.20 mg, 0.10 mmol), AgOAc (83.5 mg, 0.50 mmol), and N-methyl-2-pyrrolidone (1.0 mL) was stirred in a tube reaction covered with aluminum foil at 145 °C for 24 h under argon atmosphere. Then the reaction mixture was cooled to room temperature, and water (10 mL) was added. The mixture was extracted with ethyl acetate (3 × 15 mL), and the organic phase was dried over

Na₂SO₄ and concentrated in vacuo. After that, the residue was directly analyzed by ¹H NMR using 1,1,2,2-tetrachloroethane as the internal standard to determine the yields of products or was subjected to column chromatography on silica gel (hexane/ethyl acetate = 3:1) to give the desired products.

Procedure for a gram-scale acetoxylation reaction for synthesizing 4v.

A reaction tube was covered with aluminum foil, and a mixture of amide **1v** (1.32 g, 4.93 mmol), Cu(OAc)₂ (984.3 mg, 4.93 mmol), AgOAc (4.1 g, 24.7 mmol), NaOAc (404.3 mg, 4.93 mmol), and N-methyl-2-pyrrolidone (49.3 mL) was stirred at 145 °C for 24 h under argon atmosphere. The reaction mixture was cooled to room temperature, filtrated through Celite, and the residue was washed with ethyl acetate (200 mL). Then, water (100 mL) was added to the filtrate, and the mixture was extracted with ethyl acetate (3 × 150 mL). The organic phase was dried over Na₂SO₄ and was concentrated in vacuo. The crude mixture was subjected to column chromatography on silica gel (hexane/ethyl acetate = 3:1) to give the desired product **4v** (1.13 g, 70% yield).

Characterization data for compounds 2-(4-Methoxyphenyl)-2-methyl-N-(quinolin-8yl)propenamide (1a):

Eluent: hexane/ethyl acetate = 10:1, 52.0 mg, 95% yield, pale yellow oil. ¹H NMR (CDCl₃, 500 MHz) δ 1.76 (s, 6H), 3.82 (s, 3H), 6.95 – 6.92 (m, 2H), 7.36 (dd, *J* = 8.2, 4.2 Hz, 1H), 7.48 – 7.43 (m, 3H), 7.51 (t, *J* = 8.0 Hz, 1H), 8.08 (dd, *J* = 8.2, 1.5 Hz, 1H), 8.62 (dd, *J* = 4.2, 1.6 Hz, 1H), 8.76 (dd, *J* = 7.5, 0.9 Hz, 1H), 9.88 (s, 1H); ¹³C{¹H} NMR (CDCl₃, 126 MHz) δ 27.4, 47.9, 55.6, 114.3, 116.2, 121.4, 121.7, 127.6, 127.7, 128.1, 135.0, 136.3, 137.2, 138.9, 148.4, 158.8, 176.4; IR (KBr, ν / cm⁻¹) 3437, 2972, 2936, 2835, 1671, 1578, 1524, 1486, 1423, 1386, 1299, 1252, 1184, 1147, 1102, 1056, 1034, 908, 826, 792, 754, 732, 669; HRMS (ESI-TOF) *m/z*: [M + Na]⁺ Calcd for C₂₀H₂₀N₂O₂Na 343.1417; Found 343.1411.

2-Ethyl-2-(4-methoxybenzyl)-N-(quinolin-8-yl)butanamide (1e):

Eluent: hexane/ethyl acetate = 10:1, 35.5 mg, 59%, pale yellow oil. ¹H NMR (CDCl₃, 500 MHz) δ 1.01 (t, *J* = 7.4 Hz, 6H), 1.76 – 1.66 (m, 2H), 1.91 – 1.82 (m, 2H), 3.00 (s, 2H), 3.67 (s, 3H), 6.68 (d, *J* = 8.6 Hz, 2H), 7.07 (d, *J* = 8.5 Hz, 2H), 7.42 (dd, *J* = 8.2, 4.2 Hz, 1H), 7.50 – 7.47 (m, 1H), 7.54 (t, *J* = 7.8 Hz, 1H), 8.14 (d, *J* = 8.0 Hz, 1H), 8.75 – 8.73 (m, 1H), 8.84 (d, *J* = 7.6 Hz, 1H), 10.11 (brs, 1H); ¹³C{¹H} NMR (CDCl₃, 126 MHz) δ 8.8, 26.6, 40.0, 52.7, 55.3, 113.7, 116.5, 121.4, 121.70, 127.71, 128.2, 130.1, 131.2, 134.8, 136.4, 139.1, 148.4, 158.3, 175.4; IR (KBr, ν / cm⁻¹) 3444, 3054, 2969, 2936, 2837, 2788, 1653, 1528, 1514, 1488, 1457, 1423, 1385, 1325, 1265, 1179, 826, 793, 740, 705, 669; HRMS (ESI-TOF) *m/z*: [M + Na]⁺ Calcd for C₂₃H₂₆N₂O₂Na 385.1886; Found 385.1880.

3-(4-Methoxyphenyl)-3-methyl-1-(quinolin-8-yl)azetid-2-one (2a):

Eluent: hexane/ethyl acetate = 8:1, 16.9 mg, 53% yield, colorless oil. ¹H NMR (CDCl₃, 500 MHz) δ 1.80 (s, 3H), 3.80 (s, 3H), 4.65 (d, *J* = 7.3 Hz, 1H), 4.78 (d, *J* = 7.2 Hz, 1H), 6.95 – 6.89 (m, 2H), 7.37 (dd, *J* = 8.2, 4.1 Hz, 1H), 7.53 – 7.46 (m,

4H), 8.10 (dd, $J = 8.2, 1.7$ Hz, 1H), 8.55 (dd, $J = 6.4, 2.7$ Hz, 1H), 8.80 (dd, $J = 4.1, 1.8$ Hz, 1H); $^{13}\text{C}\{^1\text{H}\}$ NMR (CDCl_3 , 126 MHz) δ 23.8, 55.5, 58.7, 61.3, 114.3, 119.8, 121.4, 123.2, 127.0, 127.4, 129.2, 133.6, 135.2, 136.1, 140.6, 148.7, 158.8, 171.7; IR (KBr, ν / cm^{-1}) 3445, 3007, 2963, 2930, 2906, 2864, 2834, 1739, 1645, 1612, 1571, 1514, 1505, 1473, 1426, 1402, 1349, 1296, 1249, 1206, 1182, 1153, 1101, 1032, 957, 900, 826, 812, 790, 759, 736, 700, 668; HRMS (ESI-TOF) m/z : $[\text{M} + \text{Na}]^+$ Calcd for $\text{C}_{20}\text{H}_{18}\text{N}_2\text{O}_2\text{Na}$ 341.1260; Found 341.1259.

5-Methoxy-3,3-dimethyl-1-(quinolin-8-yl)indolin-2-one (3a):

Eluent: hexane/ethyl acetate = 8:1, 11.5 mg, 36% yield, colorless oil. ^1H NMR (CDCl_3 , 500 MHz) δ 1.55 (s, 3H), 1.63 (s, 3H), 3.65 (s, 3H), 5.96 (d, $J = 2.2$ Hz, 1H), 6.59 (dd, $J = 8.1, 2.2$ Hz, 1H), 7.21 (d, $J = 8.2$ Hz, 1H), 7.42 (dd, $J = 8.3, 4.1$ Hz, 1H), 7.67 (t, $J = 7.8$ Hz, 1H), 7.77 (d, $J = 7.2$ Hz, 1H), 7.94 (d, $J = 8.3$ Hz, 1H), 8.23 – 8.20 (m, 1H), 8.85 – 8.82 (m, 1H); $^{13}\text{C}\{^1\text{H}\}$ NMR (CDCl_3 , 126 MHz) δ 24.9, 25.7, 44.4, 55.7, 97.7, 106.8, 122.1, 123.1, 126.6, 128.0, 129.4, 129.9, 130.1, 132.8, 136.3, 144.6, 145.5, 151.2, 159.8, 182.6; IR (KBr, ν / cm^{-1}) 3436, 3054, 2969, 2937, 2835, 1718, 1627, 1541, 1505, 1473, 1456, 1393, 1375, 1362, 1204, 1168, 1130, 1095, 1029, 991, 939, 884, 827, 793, 749, 681; HRMS (ESI-TOF) m/z : $[\text{M} + \text{Na}]^+$ Calcd for $\text{C}_{20}\text{H}_{18}\text{N}_2\text{O}_2\text{Na}$ 341.1260; Found 341.1259.

3-(4-Chlorophenyl)-3-methyl-1-(quinolin-8-yl)azetidindione (2c):

Eluent: hexane/ethyl acetate = 8:1, 15.1 mg, 47% yield, colorless oil. ^1H NMR (CDCl_3 , 500 MHz) δ 1.80 (s, 3H), 4.67 (d, $J = 7.3$ Hz, 1H), 4.79 (d, $J = 7.3$ Hz, 1H), 7.40 – 7.32 (m, 3H), 7.55 – 7.45 (m, 4H), 8.13 – 8.07 (m, 1H), 8.55 – 8.50 (m, 1H), 8.80 (dd, $J = 4.0, 2.3$ Hz, 1H); $^{13}\text{C}\{^1\text{H}\}$ NMR (CDCl_3 , 126 MHz) δ 23.9, 58.9, 61.0, 119.9, 121.5, 123.4, 127.0, 127.8, 129.0, 129.2, 133.2, 135.0, 136.2, 140.0, 140.6, 148.8, 170.9; IR (KBr, ν / cm^{-1}) 3472, 3048, 2967, 2936, 2878, 2836, 1742, 1611, 1596, 1570, 1504, 1473, 1426, 1400, 1366, 1349, 1311, 1297, 1252, 1204, 1180, 1155, 1129, 1099, 1060, 1033, 1013, 953, 909, 850, 826, 789, 757, 733, 667, 637; HRMS (ESI-TOF) m/z : $[\text{M} + \text{Na}]^+$ Calcd for $\text{C}_{19}\text{H}_{15}\text{ClN}_2\text{O}_2\text{Na}$ 345.0765; Found 345.0764.

5-Chloro-3,3-dimethyl-1-(quinolin-8-yl)indolin-2-one (3c):

Eluent: hexane/ethyl acetate = 8:1, 14.2 mg, 44% yield, colorless oil. ^1H NMR (CDCl_3 , 500 MHz) δ 1.56 (s, 3H), 1.63 (s, 3H), 6.35 (d, $J = 1.8$ Hz, 1H), 7.04 (dd, $J = 7.9, 2.0$ Hz, 1H), 7.22 (d, $J = 7.9$ Hz, 1H), 7.44 (dd, $J = 8.3, 4.1$ Hz, 1H), 7.70 – 7.66 (m, 1H), 7.76 (dd, $J = 7.3, 1.4$ Hz, 1H), 7.96 (dd, $J = 8.2, 1.2$ Hz, 1H), 8.23 (dd, $J = 8.3, 1.6$ Hz, 1H), 8.82 (dd, $J = 4.1, 1.6$ Hz, 1H); $^{13}\text{C}\{^1\text{H}\}$ NMR (CDCl_3 , 126 MHz) δ 24.6, 25.4, 44.6, 110.5, 122.2, 122.6, 123.5, 126.6, 129.7, 129.9, 130.1, 132.3, 133.3, 134.2, 136.4, 144.4, 145.5, 151.3, 181.9; IR (KBr, ν / cm^{-1}) 3435, 3054, 2929, 1725, 1646, 1541, 1498, 1489, 1471, 1457, 1426, 1392, 1373, 1360, 1265, 1204, 1152, 1122, 1080, 939, 911, 884, 824, 809, 792, 755, 710, 693; HRMS (ESI-TOF) m/z : $[\text{M} + \text{Na}]^+$ Calcd for $\text{C}_{19}\text{H}_{15}\text{ClN}_2\text{O}_2\text{Na}$ $[\text{M} + \text{Na}]^+$ 345.0765; Found 345.0770.

3-(4-Fluorophenyl)-3-methyl-1-(quinolin-8-yl)azetidindione (2d):

Eluent: hexane/ethyl acetate = 8:1, 14.7 mg, 48% yield, colorless oil. ^1H NMR (CDCl_3 , 500 MHz) δ 1.80 (s, 3H), 4.67 (d, $J = 7.3$ Hz, 1H), 4.80 (d, $J = 7.3$ Hz, 1H), 7.09 – 7.03 (m, 2H), 7.38 (dd, $J = 8.2, 4.1$ Hz, 1H), 7.55 – 7.48 (m, 4H), 8.11 (dd, $J = 8.4, 1.6$ Hz, 1H), 8.54 (dd, $J = 7.0, 1.9$ Hz, 1H), 8.80 (dd, $J = 4.0, 1.7$ Hz, 1H); $^{13}\text{C}\{^1\text{H}\}$ NMR (CDCl_3 , 126 MHz) δ 24.0, 58.8, 61.2, 115.7 (d, $J = 21.4$ Hz), 119.9, 121.5, 123.4, 127.0, 128.0 (d, $J = 7.56$ Hz), 129.2, 135.1, 136.2, 137.3 (d, $J = 3.5$ Hz), 140.6, 148.8, 162.1 (d, $J = 247$ Hz), 171.2; IR (KBr, ν / cm^{-1}) 3468, 3066, 3008, 2966, 2922, 2866, 1741, 1652, 1609, 1596, 1571, 1506, 1474, 1426, 1403, 1350, 1302, 1263, 1226, 1154, 1093, 1034, 1015, 957, 903, 825, 804, 789, 758, 736; HRMS (ESI-TOF) m/z : $[\text{M} + \text{Na}]^+$ Calcd for $\text{C}_{19}\text{H}_{15}\text{FN}_2\text{O}_2\text{Na}$ 329.1061; Found 329.1063.

5-Fluoro-3,3-dimethyl-1-(quinolin-8-yl)indolin-2-one (3d):

Eluent: hexane/ethyl acetate = 8:1, 14.4 mg, 47% yield, colorless oil. ^1H NMR (CDCl_3 , 500 MHz) δ 1.56 (s, 3H), 1.63 (s, 3H), 6.09 (dd, $J = 9.1, 2.4$ Hz, 1H), 6.78 – 6.72 (m, 1H), 7.23 (dd, $J = 8.2, 5.4$ Hz, 1H), 7.44 (dd, $J = 8.2, 4.2$ Hz, 1H), 7.70 – 7.66 (m, 1H), 7.77 (dd, $J = 7.3, 1.4$ Hz, 1H), 7.96 (dd, $J = 8.2, 1.4$ Hz, 1H), 8.23 (dd, $J = 8.3, 1.7$ Hz, 1H), 8.83 (dd, $J = 4.1, 1.7$ Hz, 1H); $^{13}\text{C}\{^1\text{H}\}$ NMR (CDCl_3 , 126 MHz) δ 24.8, 25.5, 44.6, 98.6 (d, $J = 27.72$ Hz), 108.8 (d, $J = 22.68$ Hz), 122.2, 123.4 (d, $J = 8.82$ Hz), 126.6, 129.6, 129.9, 130.0, 131.1 (d, $J = 2.52$ Hz), 132.4, 136.4, 144.4, 145.7 (d, $J = 12.6$ Hz), 151.3, 162.8 (d, $J = 243.18$ Hz), 182.2; IR (KBr, ν / cm^{-1}) 3427, 3044, 2979, 2946, 2827, 2768, 1721, 1646, 1542, 1523, 1499, 1472, 1393, 1376, 1362, 1324, 1274, 1196, 1166, 1110, 1092, 830, 792, 729, 696, 669; HRMS (ESI-TOF) m/z : $[\text{M} + \text{Na}]^+$ Calcd for $\text{C}_{19}\text{H}_{15}\text{FN}_2\text{O}_2\text{Na}$ 329.1061; Found 329.1055.

3,3-Diethyl-4-(4-methoxyphenyl)-1-(quinolin-8-yl)azetidindione (2'e):

Eluent: hexane/ethyl acetate = 8:1, Colorless oil. ^1H NMR (CDCl_3 , 500 MHz) δ 0.82 (t, $J = 7.4$ Hz, 3H), 1.19 (t, $J = 7.4$ Hz, 3H), 1.33 – 1.25 (m, 1H), 1.61 – 1.52 (m, 1H), 2.12 – 1.99 (m, 2H), 3.69 (s, 3H), 6.08 (s, 1H), 6.72 (d, $J = 8.5$ Hz, 2H), 7.15 (d, $J = 8.5$ Hz, 2H), 7.23 (dd, $J = 8.3, 4.1$ Hz, 1H), 7.57 – 7.50 (m, 2H), 7.99 (d, $J = 8.1$ Hz, 1H), 8.35 – 8.33 (m, 1H), 8.65 (d, $J = 4.0$ Hz, 1H); $^{13}\text{C}\{^1\text{H}\}$ NMR (CDCl_3 , 126 MHz) δ 8.5, 9.2, 22.6, 25.5, 55.3, 63.7, 69.0, 113.7, 121.3, 122.4, 124.3, 126.7, 128.1, 129.2, 130.7, 133.3, 135.8, 141.5, 148.9, 158.8, 173.2; IR (KBr, ν / cm^{-1}) 3444, 2966, 2935, 2838, 2786, 1739, 1647, 1541, 1514, 1504, 1472, 1424, 1398, 1365, 1338, 1248, 1176, 1129, 1099, 1034, 827, 790, 756, 668; HRMS (ESI-TOF) m/z : $[\text{M} + \text{Na}]^+$ Calcd for $\text{C}_{23}\text{H}_{24}\text{N}_2\text{O}_2\text{Na}$ 383.1730; Found 383.1734.

3-Methyl-3-propyl-1-(quinolin-8-yl)azetidindione (2i):

Eluent: hexane/ethyl acetate = 8:1, 19.6 mg, 93% yield, colorless oil. ^1H NMR (CDCl_3 , 500 MHz) δ 0.97 (t, $J = 7.3$ Hz, 3H), 1.48 – 1.39 (m, 4H), 1.64 – 1.52 (m, 1H), 1.75 – 1.70 (m, 2H), 4.24 (d, $J = 7.3$ Hz, 1H), 4.40 (d, $J = 7.3$ Hz, 1H), 7.36 (dd, $J = 8.3, 4.1$ Hz, 1H), 7.51 – 7.45 (m, 2H), 8.08 (dd, $J = 8.3, 1.7$ Hz, 1H), 8.49 (dd, $J = 6.0, 3.0$ Hz, 1H), 8.79 (dd, $J = 4.1, 1.7$ Hz, 1H); $^{13}\text{C}\{^1\text{H}\}$ NMR (CDCl_3 , 126 MHz) δ 14.7, 18.4, 19.8, 37.4, 55.6, 58.8, 119.6, 121.4, 122.9, 126.9, 129.1, 135.3, 136.1, 140.5, 148.6, 173.7; IR (KBr, ν / cm^{-1}) 3458, 2959, 2929, 2904, 2871, 2845, 1743, 1637, 1612, 1595, 1570, 1527, 1504, 1474, 1426, 1401, 1365, 1348,

1200, 1188, 1151, 1133, 1107, 1060, 1030, 971, 905, 826, 814, 790, 758, 641; HRMS (ESI-TOF) m/z : $[M + Na]^+$ Calcd for $C_{16}H_{18}N_2ONa$ 277.1311; Found 277.1306.

ASSOCIATED CONTENT

Supporting Information

Experimental procedures, compound characterization data and spectra, details of calculation (PDF)

This material is available free of charge via the Internet at <http://pubs.acs.org>.

AUTHOR INFORMATION

Corresponding Author

*E-mail: bencan.tang@nottingham.edu.cn

*E-mail: kuninobu@mol.f.u-tokyo.ac.jp

*E-mail: zhenw@lzu.edu.cn

Author Contributions

‡ Y. Y., F. C. and L. Y. contributed equally.

Notes

The authors declare no competing financial interest.

ACKNOWLEDGMENT

Financial support was provided by Grant-in-Aid for Scientific Research (B) from the Ministry of Education, Culture, Sports, Science, and Technology of Japan, and the Recruitment Program of Global Experts (1000 Talents Plan) and the Fundamental Research Funds for the Central Universities (lzujbky-2019-ct08). The authors (BT & LB) acknowledge the financial support from Ministry of Science and Technology of the People's Republic of China under funding figure National Key R&D Program of Intergovernmental Kay Projects (Grant No. 2018YFE0101700), the National Natural Science Foundation of China (21502101), the Natural Science Foundation of Ningbo (2017A610070), the International Doctoral Innovation Centre, Ningbo Education Bureau, Ningbo Science and Technology Bureau, and the University of Nottingham for the use of High Performance Computing Facility.

REFERENCES

- Suess, A. M.; Ertem, M. Z.; Cramer, C. J.; Stahl, S. S. Divergence between Organometallic and Single-Electron-Transfer Mechanisms in Copper(II)-Mediated Aerobic C–H Oxidation. *J. Am. Chem. Soc.* **2013**, *135*, 9797–9804.
- Chen, F.; Shen, T.; Cui, Y.; Jiao, N. 2,4- vs 3,4-Disubstituted Pyrrole Synthesis Switched by Copper and Nickel Catalysts. *Org. Lett.* **2012**, *14*, 4926–4929.
- Su, Y.; Sun, X.; Wu, G.; Jiao, N. Catalyst-Controlled Highly Selective Coupling and Oxygenation of Olefins: A Direct Approach to Alcohols, Ketones, and Diketones. *Angew. Chem. Int. Ed.* **2013**, *52*, 9808–9812.
- Chen, P.-H.; Xu, T.; Dong, G. Divergent Syntheses of Fused b-Naphthol and Indene Scaffolds by Rhodium-Catalyzed Direct and Decarbonylative Alkyne–Benzocyclobutenone Couplings. *Angew. Chem. Int. Ed.* **2014**, *53*, 1674–1678.
- Takemura, N.; Kuninobu, Y.; Kanai, M. Copper-Catalyzed C–H Alkoxylation of Azoles. *Org. Lett.* **2013**, *15*, 844–847.
- Li, B.; Guo, S.; Zhang, J.; Zhang, X.; Fan, X. Selective Access to 3-Cyano-1H-indoles, 9H-Pyrimido[4,5-b]indoles, or 9H-Pyrido[2,3-b]indoles through Copper-Catalyzed One-Pot Multicomponent Cascade Reactions. *J. Org. Chem.* **2015**, *80*, 5444–5456.
- Jiang, Y.; Feng, Y.-Y.; Zou, J.-X.; Lei, S.; Hu, X.-L.; Yin, G.-F.; Tan, W.; Wang, Z. Brønsted Base-Switched Selective Mono- and Di-thiolation of Benzamides via Copper Catalysis. *J. Org. Chem.* **2019**, *84*, 10490–10500.
- Wang, Z.; Ni, J.; Kuninobu, Y.; Kanai, M. Copper-Catalyzed Intramolecular C(sp³)-H and C(sp²)-H Amidation by Oxidative Cyclization. *Angew. Chem. Int. Ed.* **2014**, *53*, 3496–3499.
- Slightly after our publication, Ge's group reported a similar reaction, please see: Wu, X.; Zhao, Y.; Zhang, G.; Ge, H. Copper-Catalyzed Site-Selective Intramolecular Amidation of Unactivated C(sp³)-H Bonds. *Angew. Chem. Int. Ed.* **2014**, *53*, 3706–3710.
- Wang, Z.; Kuninobu, Y.; Kanai, M. Copper-Mediated Direct C(sp³)-H and C(sp²)-H Acetoxylation. *Org. Lett.* **2014**, *16*, 4790–4793.
- Almost at the same time, Ge's group reported a similar reaction, please see: Wu, X.; Zhao, Y.; Ge, H. Copper-Promoted Site-Selective Acyloxylation of Unactivated C(sp³)-H Bonds. *Chem. Asian J.* **2014**, *9*, 2736–2739.
- Gandeepan, P.; Müller, T.; Zell, D.; Cera, G.; Warratz, S.; Ackermann, L. 3d Transition Metals for C–H Activation. *Chem. Rev.* **2019**, *119*, 2192–2452.
- Chen, X.; Hao, X.-S.; Goodhue, C. E.; Yu, J.-Q. Cu(II)-Catalyzed Functionalizations of Aryl C–H Bonds Using O₂ as an Oxidant. *J. Am. Chem. Soc.* **2006**, *128*, 6790–6791.
- Jin, J.; Wen, Q.; Lu, P.; Wang, Y. Copper-catalyzed cyanation of arenes using benzyl nitrile as a cyanide anion surrogate. *Chem. Commun.* **2012**, *48*, 9933–9935.
- Evano, G.; Blanchard, N. *Copper-Mediated Cross-Coupling Reactions*; Wiley: Hoboken, New Jersey, 2014.
- Modern Organocopper Chemistry*; Krause, N., Ed.; Wiley-VCH: Weinheim, Germany, 2002.
- Alexakis, A.; Krause, N.; Woodward, S. *Copper-Catalyzed Asymmetric Synthesis*; Wiley-VCH: Weinheim, Germany, 2014.
- A comparison of the electronic effects of "electrophilic" C–H activation by Pd II and other more-classical electrophiles, please see: Stock, L. M.; Tse, K.-t.; Vorvick, L. J.; Walstrum, S. A. Palladium(II) acetate catalyzed aromatic substitution reaction. *J. Org. Chem.* **1981**, *46*, 1757–1759.
- A. D. Ryabov, I. K. Sakodinskaya, A. K. Yatsimirsky, Kinetics and mechanism of ortho-palladation of ring-substituted NN-dimethylbenzylamines. *J. Chem. Soc. Dalton Trans.* **1985**, *14*, 2629–2638.
- Karig, G.; Moon, M. T.; Thasana, N.; Gallagher, T. C–H Activation and Palladium Migration within Biaryls under Heck Reaction Conditions. *Org. Lett.* **2002**, *4*, 3115–3118.
- Davies, D. L.; Donald, S. M. A.; Macgregor, S. A. Computational Study of the Mechanism of Cyclometalation by Palladium Acetate. *J. Am. Chem. Soc.* **2005**, *127*, 13754–13755.
- García-Cuadrado, D.; Braga, A. A. C.; Maseras, F.; Echavarren, A. M. Proton Abstraction Mechanism for the Palladium-Catalyzed Intramolecular Arylation. *J. Am. Chem. Soc.* **2006**, *128*, 1066–1067.
- Gorelsky, S. I.; Lapointe, D.; Fagnou, K. Analysis of the Concerted Metalation-Deprotonation Mechanism in Palladium-Catalyzed Direct Arylation Across a Broad Range of Aromatic Substrates. *J. Am. Chem. Soc.* **2008**, *130*, 10848–10849.
- Balcells, D.; Clot, E.; Eisenstein, O. C–H Bond Activation in Transition Metal Species from a Computational Perspective. *Chem. Rev.* **2010**, *110*, 749–823.
- Sun, H. Y.; Gorelsky, S. I.; Stuart, D. R.; Campeau, L. C.; Fagnou, K. Mechanistic analysis of azine N-oxide direct arylation: evidence for a critical role of acetate in the Pd(OAc)₂ precatalyst. *J. Org. Chem.* **2010**, *75*, 8180–8189.
- Ackermann, L. Carboxylate-Assisted Transition-Metal-Catalyzed C–H Bond Functionalizations: Mechanism and Scope. *Chem. Rev.* **2011**, *111*, 1315–1345.
- Gorelsky, S. I.; Lapointe, D.; Fagnou, K. Analysis of the Palladium-Catalyzed (Aromatic)C–H Bond Metalation–

Deprotonation Mechanism Spanning the Entire Spectrum of Arenes. *J. Org. Chem.* **2012**, *77*, 658–668.

[28] Chen, C.; Hao, Y.; Zhang, T.-Y.; Pan, J.-L.; Ding, J.; Xiang, H.-Y.; Wang, M.; Ding, T.-M.; Duan, A.; Zhang, S.-Y. Computational and experimental studies on copper-mediated selective cascade C–H/N–H annulation of electron-deficient acrylamide with arynes. *Chem. Commun.* **2019**, *55*, 755–758.

[29] Simmons, E. M.; Hartwig, J. F. On the Interpretation of Deuterium Kinetic Isotope Effects in C–H Bond Functionalizations by Transition-Metal Complexes. *Angew. Chem. Int. Ed.* **2012**, *51*, 3066–3072.

[30] Lafrance, M.; Fagnou, K. Palladium-Catalyzed Benzene Arylation: Incorporation of Catalytic Pivalic Acid as a Proton Shuttle and a Key Element in Catalyst Design. *J. Am. Chem. Soc.* **2006**, *128*, 16496–16497.

[31] Stuart, D. R.; Fagnou, K. The Catalytic Cross-Coupling of Unactivated Arenes. *Science* **2007**, *316*, 1172–1175.

[32] García-Cuadrado, D.; de Mendoza, P.; Braga, A. A. C.; Maseras, F.; Echavarren, A. M. Proton-Abstraction Mechanism in the Palladium-Catalyzed Intramolecular Arylation: Substituent Effects. *J. Am. Chem. Soc.* **2007**, *129*, 6880–6886.

[33] Lafrance, M.; Gorelsky, S. I.; Fagnou, K. High-Yielding Palladium-Catalyzed Intramolecular Alkane Arylation: Reaction Development and Mechanistic Studies. *J. Am. Chem. Soc.* **2007**, *129*, 14570–14571.

[34] Because Cu_2CO_3 is quite unstable, the experiments were carried out using $\text{Cu}_2(\text{OH})_2\text{CO}_3$.

[35] Uemura, T.; Imoto, S.; Chatani, N. Amination of the Ortho C–H Bonds by the $\text{Cu}(\text{OAc})_2$ -mediated Reaction of 2-Phenylpyridines with Anilines. *Chem. Lett.* **2006**, *35*, 842.

[36] Please see the full references for Gaussian 09 in the Electronic supplementary materials.

[37] Takamatsu, K.; Hayashi, Y.; Kawauchi, S.; Hirano, K.; Miura, M. Copper-Catalyzed Regioselective C–H Amination of Phenol Derivatives with Assistance of Phenanthroline-Based Bidentate Auxiliary. *ACS Catal.* **2019**, *9*, 5336–5344.

[38] Examples of Ag assisted C–H activation: Y. F. Yang, P. Liu, D. Leow, T. Y. Sun, P. Chen, X. Zhang, J. Q. Yu, Y. D. Wu, K. N. Houk. Palladium-Catalyzed Meta-Selective C–H Bond Activation with a Nitrile-Containing Template: Computational Study on Mechanism and Origins of Selectivity. *J. Am. Chem. Soc.* **2014**, *136*, 344–355.

[39] Fang, L.; Saint-Denis, T. G.; Taylor, B. L. H.; Ahlquist, S.; Hong, K.; Liu, S.; Han, L.; Houk, K. N.; Yu, J.-Q. Experimental and Computational Development of a Conformationally Flexible Template for the meta-C–H Functionalization of Benzoic Acids. *J. Am. Chem. Soc.* **2017**, *139*, 10702–10714.

[40] Bay, K. L.; Yang, Y.-F.; Houk, K. N. Multiple roles of silver salts in palladium-catalyzed C–H activations. *J. Organomet. Chem.* **2018**, *864*, 19–25.

[41] Ruan, G.-Y.; Qi, Z.-H.; Zhang, Y.; Liu, W.; Wang, Y. Mechanistic insight into Cu/Ag-cocatalyzed C–H activation of arenes with oxygen as the terminal oxidant. *RSC Adv.* **2016**, *6*, 35855–35858.

[42] Example for intramolecular acetoxylation pathways: Zhang, J.; Chen, H.; Wang, B.; Liu, Z.; Zhang, Y. Copper-Mediated Aryloxylation and Vinyloxylation of $\beta\text{-C}(\text{sp}^3)\text{-H}$ Bond of Propionamides with Organosilanes. *Org. Lett.* **2015**, *17*, 2768–2771.

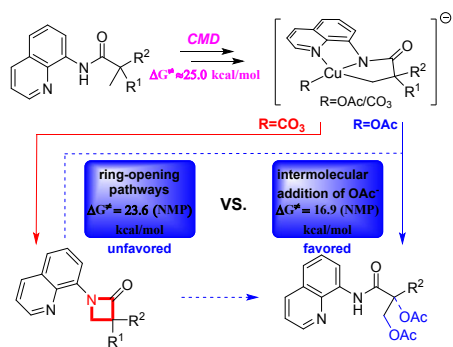
[43] Rao, W.-H.; Shi, B.-F. Copper(II)-Catalyzed Direct Sulfonylation of $\text{C}(\text{sp}^2)\text{-H}$ Bonds with Sodium Sulfinates. *Org. Lett.* **2015**, *17*, 2784–2787.

[44] An example for $\text{Cu}(\text{CO}_3)$ -species-involved CMD pathway, please see: ref. 1. An example for $\text{Pd}(\text{CO}_3)$ -species-involved CMD pathway, please see: Zhang, S.-Y.; Li, Q.; He, G.; Nack, W. A.; Chen, G. Stereoselective Synthesis of β -Alkylated α -Amino Acids via Palladium-Catalyzed Alkylation of Unactivated Methylene $\text{C}(\text{sp}^3)\text{-H}$ Bonds with Primary Alkyl Halides. *J. Am. Chem. Soc.* **2013**, *135*, 12135–12141.

[45] Xiong, H. Y.; Besset, T.; Cahard, D.; Pannecoucke, X. Palladium(II)-Catalyzed Directed Trifluoromethylthiolation of Unactivated $\text{C}(\text{sp}^3)\text{-H}$ Bonds. *J. Org. Chem.* **2015**, *80*, 4204–4212.

[46] Wu, X. S.; Zhao, Y.; Ge, H. B. Nickel - Catalyzed Site - Selective Amidation of Unactivated $\text{C}(\text{sp}^3)\text{-H}$ Bonds. *Chem. Eur. J.* **2014**, *20*, 9530 – 9533.

[47] Wu, X. S.; Zhao, Y.; Zhang, G. W.; Ge, H. B. Copper - Catalyzed Site - Selective Intramolecular Amidation of Unactivated $\text{C}(\text{sp}^3)\text{-H}$ Bonds. *Angew. Chem. Int. Ed.* **2014**, *53*, 3706 – 3710.



Insert Table of Contents artwork here
